23. Read, W. G. *et al.* Upper-tropospheric water vapor from UARS MLS. *Bull. Am. Met. Soc.* **76,** 2381–2389 (1995); also at ⟨http://mls. jpl. nasa. gov/joe/h2o_uptrop_djf_jja. html⟩.
24. Susskind, J. *et al.* Characteristics of the TOVS Pathfinder Path A dataset. *Bull. Am. Met. Soc.* **78,** 1449–1472 (1997).
25. Randel, D. L. *et al.* A new global water vapor dataset. *Bull. Am. Meteorol. Soc.* **77,** 1233–1246 (1996).
26. Latham, J. & Christian, H. Satellite measurements of global lightning. *Q. J. R. Meteorol. Soc.* **124,** 1771–1773 (1998).
27. Schumann, W. O. Über die strahlungslosen Eigenschwingungen einer leitenden Kugel, die von einer Luftschicht und einer Ionosphärenhülle umgeben ist. *Z. Naturforsch.* **7a,** 149–162 (1952).
28. Heckman, S. J., Williams, E. & Boldi, B. Total global lightning inferred from Schumann Resonance measurements. *J. Geophys. Res.* **103,** 31775–31779 (1998).
29. Fraser-Smith, A. C. *et al.* in *Environmental and Space Electrodynamics* (ed. Kikuchi, H.) 191–200 (Springer, Tokyo, 1991).
30. Price, C. *et al.* Possible implications of global climate change on global lightning distributions and frequencies. *J. Geophys. Res.* **99,** 10823–10831 (1994).

Acknowledgements

I would like to thank T. Fraser-Smith for the use of the Antarctica ELF data used in this study and M. Füllekrug for making available the California data in Fig. 3 on the Internet. Part of this research was supported by the Israel-US Binational Science Foundation, and the European Community International Association for the promotion of co-operation with scientists from the New Independent States of the former Soviet Union (INTAS) programme.

Correspondence and requests for materials should be addressed to C. P. (e-mail: cprice@flash.tau.ac.il).

Melting of the Earth's lithospheric mantle inferred from protactinium–thorium–uranium isotopic data

Yemane Asmerom*, Hai Cheng†, Rebecca Thomas†, Marc Hirschmann† & R. Lawrence Edwards†

** Department of Earth and Planetary Sciences, University of New Mexico, Albuquerque, New Mexico 87131, USA*
† Department of Geology and Geophysics, University of Minnesota, Minneapolis, Minnesota 55455, USA

The processes responsible for the generation of partial melt in the Earth's lithospheric mantle and the movement of this melt to the Earth's surface remain enigmatic, owing to the perceived difficulties in generating large-degree partial melts at depth and in transporting small-degree melts through a static lithosphere[1]. Here we present a method of placing constraints on melting in the lithospheric mantle using ^{231}Pa–^{235}U data obtained from continental basalts in the southwestern United States and Mexico. Combined with ^{230}Th–^{238}U data[2,3], the ^{231}Pa–^{235}U data allow us to constrain the source mineralogy and thus the depth of melting of these basalts. Our analysis indicates that it is possible to transport small melt fractions—of the order of 0.1%—through the lithosphere, as might result from the coalescence of melt by compaction[4] owing to melting-induced deformation[5]. The large observed ^{231}Pa excesses require that the timescale of melt generation and transport within the lithosphere is small compared to the half-life of ^{231}Pa (~32.7 kyr). The ^{231}Pa–^{230}Th data also constrain the thorium and uranium distribution coefficients for clinopyroxene in the source regions of these basalts to be within 2% of one another, indicating that in this setting ^{230}Th excesses are not expected during melting at depths shallower than 85 km.

Basalts from old continental settings are ideally suited for the study of lithospheric melting processes because they allow discrimination between lithospheric and asthenospheric mantle melts using Nd isotopes[2]. The samples for this study are well-characterized North American continental basalts for which Nd and Th isotopic compositions and trace-element abundances have previously been reported[2,3]. The two groups of samples consist of: (1) asthenospheric mantle-derived alkali basalts (high ϵ_{Nd} values of around +5) from the Pinacate volcanic field, Mexico, and the Potrillo volcanic field in the southern Rio Grande Rift, USA; and (2) lithospheric mantle-derived (low ϵ_{Nd} values of around 0) alkali basalts from the San Francisco volcanic field, Colorado Plateau, and a tholeiite from the Zuni Bandera volcanic field in the Colorado Plateau–Rio Grande transition (Fig. 1).

As shown previously[2,3], the ^{230}Th/^{238}U enrichments in continental basalts correlate with their inferred mantle sources. The lavas with low ϵ_{Nd} values, thought to be derived from the lithospheric mantle, have equilibrium (^{230}Th/^{238}U) values, whereas lavas with high ϵ_{Nd} values, presumed to be derived from the asthenosphere, have large ^{230}Th enrichments. Initial (^{231}Pa/^{235}U) values in asthenospheric alkalic lavas (Table 1) fall in a narrow range from 2.33 ± 14 to 2.44 ± 15 (the uncertainty is mostly related to uncertainty in age), whereas the lithospheric mantle values are 2.00 ± 3 and 2.02 ± 2 for the alkali basalts and 1.44 ± 3 for the tholeiite.

The salient feature of the Pa data is that despite significant differences in geodynamic setting and other geochemical characteristics, all of the samples, and particularly the alkali olivine basalts, have significant (^{231}Pa/^{235}U) excesses. This is true both for samples that show large (^{230}Th/^{238}U) excesses and for those that are in secular equilibrium with respect to (^{230}Th/^{238}U). A continental basalt from the Snake River Plain that has substantial Pa excess [(^{231}Pa/^{235}U) = 1.7] but that is near secular equilibrium with respect to ^{230}Th—(^{230}Th/^{238}U) = 1.04—was also reported[6].

Alkali olivine basalts (AOBs) have significantly greater Pa enrichments than the one tholeiite analysed in this study. Similar differences between tholeiite and alkali basalts are observed in other settings[6]. As the AOBs are probably the result of smaller degrees of melting than the tholeiite[2,3], this is the expected relationship if Pa enrichment is caused by melting. The limited available data do not completely exclude exotic enrichment processes such as metasomatism, but here we will assume that the data are most probably explained by melting processes.

The coupled ^{230}Th and ^{231}Pa excesses observed in the alkali basalts from the Pinacate volcanic field and the Potrillo volcanic field, which are derived from asthenospheric mantle[2,3,7–9], may be explained by the melting of upwelling depleted (high ϵ_{Nd}) mantle, similar to the reason for excesses in MORB and ocean island

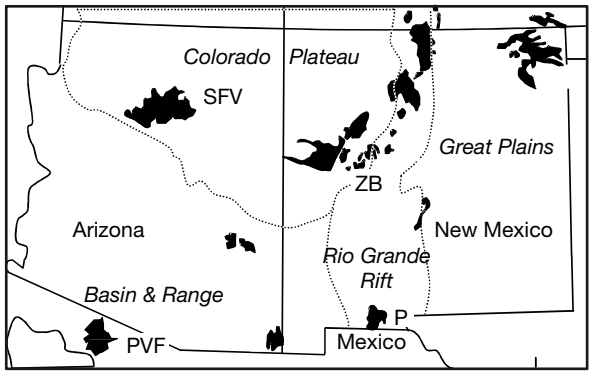

Figure 1 A general tectonic map of the study region. Shown is the Colorado Plateau, a stable part of cratonic North America (with a thick lithosphere), bounded by the Rio Grande Rift and the Basin and Range Province, USA and Mexico (regions with attenuated lithosphere). The four sample localities are: (1) the Pinacate volcanic field (PVF), Mexico (samples 92-03 and 92-04); (2) the Potrillo volcanic field (P), southern Rio Grande Rift, USA (95-06), both with highly attenuated lithosphere; (3) the San Francisco volcanic field (SFV), Colorado Plateau (92-07, 92-08); and (4) the Zuni Bandera volcanic field (ZB, 95-04), a transitional zone with attenuated lithosphere. Other Cenozoic volcanic fields are shown for context.

© 2000 Macmillan Magazines Ltd

basalts[10–12]. The large ^{231}Pa enrichment ((^{231}Pa/^{235}U) values of up to 2.00) with no ^{230}Th enrichment in the lithosphere-derived basalts is a surprising discovery. As we will show below, it is not possible to generate significant ^{231}Pa enrichments while still maintaining secular equilibrium ^{230}Th values in a garnet peridotite source using either batch melting or dynamic melting models. Thus, these data require melting in a source without garnet. This conclusion, based on combined ^{231}Pa and ^{230}Th data, is supported by previous inferences[3], attributing the lack of ^{230}Th enrichment to melting within the spinel lherzolite field. Moreover, xenolith and geophysical data from this part of the Colorado Plateau are supportive of a spinel lherzolite lithospheric mantle. In the Colorado Plateau the depth to the lithosphere–asthenosphere boundary varies from less than 60 km near the margins of the Plateau to 110 km at the centre[13]. Although xenoliths from the central part of the Plateau include garnet peridotites, those closer to the margin in settings similar to the San Francisco volcanic field consist of spinel lherzolites[14]. The lithospheric mantle at the study site is clearly within the stability field of spinel lherzolite. Melting is likely to occur at the base of the lithosphere, as a result of basal heating. As a result, the portion of the lithosphere that had partially melted is probably located beneath the present-day seismic lithosphere–asthenosphere boundary[13] (about 60 km), but above the stability of garnet peridotite[15] (less than 85 km).

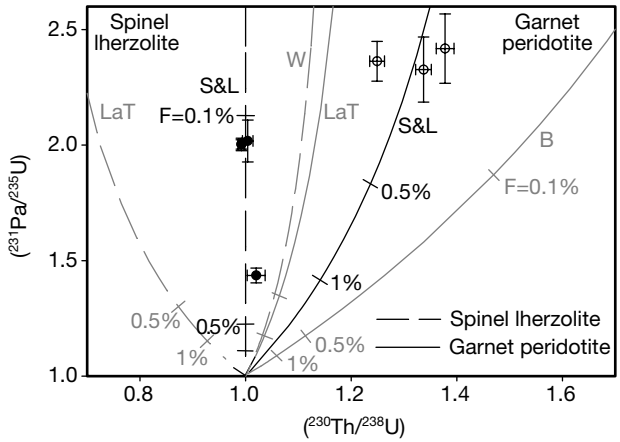

Figure 2 (^{231}Pa/^{235}U) versus (^{230}Th/^{238}U) diagram, showing our age-corrected values. Lithospheric mantle-derived basalts, with Nd isotopic values near bulk Earth, $\epsilon_{Nd} \approx 0$, are shown in filled symbols[2,3] while those with high ϵ_{Nd} values, derived from an asthenospheric source[2,3,7–9], are shown with unfilled symbols. The plotted activity ratios are decay-corrected (initial) values. The uncertainties reflect both measurement errors and uncertainties associated with ages of the samples. *F*, degree of melting. All samples are alkali basalts, except for one tholeiitic basalt (95-04) with (^{231}Pa/^{235}U) = 1.4. We note that all of the samples, including the tholeiite, are enriched in ^{231}Pa. Samples with low ϵ_{Nd} values are in secular equilibrium with respect to ^{230}Th, whereas those with high ϵ_{Nd} values have large ^{230}Th enrichments. The difference in ^{230}Th enrichment is attributed to difference in source mineralogy (spinel peridotite versus garnet peridotite, respectively[2,3]). Also shown are ^{231}Pa–^{230}Th enrichment trends for simple batch melting of spinel lherzolite (dashed lines) and garnet peridotite (solid lines) sources, using some of the published U–Th *D*-values for clinopyroxene (cpx) and garnet (gt). There are no experimental data for the *D*-value for Pa; it is inferred to be in the range of 10^{-5} (see ref. 18). S&L, Salters and Longhi[19] (dark lines); W, Wood *et al.*[20]; B, Beattie[16]; LaT, LaTourette and Burnett[21] and LaTourette *et al.*[17] *D*-value determinations by other workers fall in between the extreme values. Considering these models, the only way to get large ^{231}Pa enrichments while maintaining secular equilibrium ^{230}Th is to melt a spinel lherzolite source with $D_{Th}^{cpx}/D_{U}^{cpx} \approx 1$, consistent with the data of ref. 19. We used D_{Th}^{cpx} and D_{U}^{cpx} for clinopyroxene with a wollastonite mole fraction of about 0.5. The bulk composition of clinopyroxene is estimated from analyses of lithospheric mantle-derived clinopyroxene from the study region[27]. The alkali basalts with no ^{230}Th enrichment require melting of a spinel lherzolite with *F* values in the range of 0.1%, and larger *F* values (about 0.3%) for tholeiite. The samples with coupled ^{231}Pa–^{230}Th enrichments fit the simple batch melting of a garnet peridotite ($F \approx 0.4\%$), although dynamic melting (Fig. 3) is most likely to be relevant here.

Table 1 Protactinium, thorium and uranium data

Sample	Age (kyr)*	^{238}U (ng g^{-1})	(^{230}Th/^{238}U)	(^{230}Th/^{238}U)$_i$†	Pa (fg g^{-1})	(^{231}Pa/^{235}U)	(^{231}Pa/^{235}U)$_i$†	(^{234}U/^{238}U)
Asthenospheric mantle melts ($\epsilon_{Nd} \approx 5$)								
95-06 (II) [P]	20	1,127 ± 1	1.207 ± 13	1.249 ± 14	699 ± 24	1.893 ± 64	2.36 ± 86	1.006 ± 6
95-06 (I)		1,126 ± 1			672 ± 14	1.823 ± 38		0.997 ± 5
92-03 (II) [PVF]	~10	904 ± 1	1.307 ± 7	1.337 ± 15	615 ± 11	2.074 ± 36	2.327 ± 141	1.001 ± 6
92-03 (I)		905 ± 1			626 ± 44	2.110 ± 148		1.006 ± 5
92-04 (II) [PVF]	~10	848 ± 1	1.345 ± 9	1.378 ± 17	597 ± 9	2.148 ± 33	2.418 ± 150	1.003 ± 9
92-04 (I)		848 ± 1			596 ± 39	2.146 ± 141		1.007 ± 7
Lithospheric mantle melts ($\epsilon_{Nd} \approx 0$)								
92-07 [SFV]	0.80	1,095 ± 1	0.992 ± 5	0.992 ± 5	712 ± 10	1.986 ± 27	2.003 ± 27	0.999 ± 7
92-07§		1,102			714		2.003 ± 20	
92-07§		1,102			714		1.99 ± 20	
92-08 (II) [SFV]	0.80	1,030 ± 1	1.004 ± 10	1.004 ± 10	676 ± 31	2.001 ± 91	2.001 ± 91	1.002 ± 9
92-08 (I)		1,028 ± 1			668 ± 62	1.983 ± 185		
95-04 [ZB]	3.0	697 ± 1	1.019 ± 16	1.020 ± 17	276 ± 6	1.409 ± 32	1.436 ± 32	0.997 ± 8
Table Mountain Latite Standard								
Minnesota data		10,660 ± 12	1.002 ± 5		3,500 ± 25	1.002 ± 7		1.002 ± 1
LANL data‡		10,425	1.003 ± 7		3,415	≡1.000		
		10,474	0.996 ± 8		3,433	≡1.000		

Th isotopic analyses were done at the University of New Mexico[2] and the University of Minnesota[3]. The Pa chemistry and mass spectrometry were done at the University of Minnesota. See refs 28 and 29 for Pa separation and mass spectrometry, and refs 2 and 3 for silicate dissolution. Ratios in parentheses are activity ratios. Uncertainties on measured ratios are 2σ of the mean analytical errors. Approximate ϵ_{Nd} values are from refs 2 and 3, in which measurements for all samples except 92-03 can be found.

* See refs 2 and 3 for sources of ages.

† Uncertainties in the initial ratios reflect both analytical errors of the measured values, and age uncertainties. The large errors on the initials for 92-03 and 92-04 are due to assigning 50% error on the ages. Given the large Pa excesses in the samples, any uncertainties in initial ratios are not crucial to the interpretations in this paper. The markedly lower (^{231}Pa/^{235}U) value for the tholeiitic basalt (95-04) is not related to post-eruption decay because the young age of the tholeiite, 3,000 years, is well constrained from ^{14}C and ^{3}He dating.

‡ The (^{231}Pa/^{235}U) ratio data for the Los Alamos Table Mountain Latite[6,28] is fixed at 1.000 as it was used to calibrate their spike.

§ U and Pa in 92-07 were analysed at Los Alamos National Labs (LANL) in replicate[6]. See refs 3 and 29 for decay constants of U, Th and Pa isotopes. See legend to Fig. 1 for abbreviations in square brackets.

© 2000 Macmillan Magazines Ltd

The observed Pa and Th isotope results can be compared to simple models for melting of peridotite. In Fig. 2 the data are compared to the results of batch melting of garnet peridotite (12% clinopyroxene (cpx), 8% garnet) and spinel lherzolite (15% cpx) lithologies, using a variety of published experimental Th and U D-values and estimates of Pa D-values[16–19]. (The D value (distribution coefficient) is the ratio of the concentration of an element in a solid phase over its concentration in melt.) The calculations show that the lavas with large ^{231}Pa excesses but no ^{230}Th enrichment are inconsistent with partial melting of garnet peridotite. Using any of the available D-values, when melting a garnet peridotite, any significant enrichment in ^{231}Pa results in a coupled enrichment of ^{230}Th. Figure 2 also shows that even if the source is free of garnet (spinel lherzolite) only the D-values of ref. 19 give melts with large ^{231}Pa enrichment and no Th–U fractionation, within measurement error; $(^{230}\mathrm{Th}/^{238}\mathrm{U}) \approx 1$.

The ratio of experimentally determined U–Th D-values for clinopyroxene, $D_{\mathrm{Th}}^{\mathrm{cpx}}/D_{\mathrm{U}}^{\mathrm{cpx}}$, vary from less than one[20] to as high as 2.2 (ref. 21), and vary with composition[18] and pressure[20]. Our combined Th–Pa data may provide a robust constraint on $D_{\mathrm{Th}}^{\mathrm{cpx}}/D_{\mathrm{U}}^{\mathrm{cpx}}$. For simple batch melting of a source initially in secular equilibrium, assuming that $D_{\mathrm{Pa}} \approx 0$ and degree of melting, F, is small (about 0.1%), $\frac{D_{\mathrm{Th}}}{D_{\mathrm{U}}} = \frac{(B-A)}{A(B-1)}$, where $\mathrm{A} = (\frac{^{230}\mathrm{Th}}{^{238}\mathrm{U}})$ and $\mathrm{B} = (\frac{^{231}\mathrm{Pa}}{^{235}\mathrm{U}})$. For alkali basalts derived from the lithosphere, accounting for analytical errors on the two samples (92-07, 92-08) analysed, the weighted average of the alkali basalt source region $D_{\mathrm{Th}}/D_{\mathrm{U}}$ implied by the Pa–Th–U data is 1.012 ± 0.012 (2σ). The Pa–Th–U data for the one tholeiite measured indicates a source-region $D_{\mathrm{Th}}/D_{\mathrm{U}}$ value of 0.935 ± 0.106. The combined data yield a $D_{\mathrm{Th}}/D_{\mathrm{U}}$ value of 1.011 ± 0.012 (assuming that the tholeiite and alkali basalts share the same source region).

We observed lavas ranging in composition from tholeiites to alkali basalts that show no measurable Th excesses, but large ^{231}Pa enrichment, suggesting that the $D_{\mathrm{Th}}^{\mathrm{cpx}}/D_{\mathrm{U}}^{\mathrm{cpx}}$ is within 1% of unity, at least for these settings. Suggestions, based on theoretical considerations and limited experimental data[20], that $D_{\mathrm{Th}}^{\mathrm{cpx}}/D_{\mathrm{U}}^{\mathrm{cpx}}$ may be lower than one at pressures similar to those in the source regions of the samples we derived from the lithospheric mantle, are not supported by our data.

For the lithospheric mantle-derived melts (no ^{230}Th enrichment) very small degrees of melting (F-values in the range of 0.1%) are required to generate the observed ^{231}Pa excesses (Fig. 2, curve from ref. 19). Such small extents of melting are broadly compatible with extents of melting for these lavas implied by concentrations of other incompatible trace elements such as La and Nd in the lavas [La ≈ 100 and Nd ≈ 30 times the chondritic values][2]. For example, using the D-values of ref. 22, these extents of melting imply enrichments relative to their source of about 100–120 for La and about 35 for Nd. Although more complicated processes than batch melting[23,24] may be responsible for the observed ^{231}Pa excesses, all viable models that explain these data would require melting or melt transport at porosities of around 0.1% (Fig. 3).

One possibility is that significant separation between Pa and U may be enhanced by chromatographic separation during percolation through the lithosphere[25]. In such a process the melts ascend but the solid mantle does not upwell, and thus percolating melts are able to exchange with mantle that has not melted recently and therefore may have a larger Pa/U ratio than that of upwelling, partially melting mantle. If it occurs at sufficiently low porosity, such percolative exchange may be efficient at generating ^{231}Pa over ^{235}U excesses.

For samples derived from the asthenospheric mantle with coupled Th and Pa enrichment, both static and dynamic melting models[23,24,26] may be applicable. Batch melting of garnet peridotite with a maximum extent of melting of about 0.4% can approximate the calculated Pa–Th–U systematics of these rocks (Fig. 2). More importantly, partial melting of upwelling mantle is most probably approximated by ingrowth models, allowing for larger (about 3%) effective degrees of partial melting (Fig. 3). For example, the data are well matched by some dynamic models[23,26], and by an equilibrium porous flow model[24] as illustrated in Fig. 3, provided that the upwelling rate is on the order of 1 cm yr^{-1} or less.

Our data place strong constraints on the processes by which melting and melt extraction occur within the heated lithospheric mantle. The large observed ^{231}Pa excesses require that the timescale of melt generation and transport within the lithosphere is small compared to the half-life of ^{231}Pa (about 32.7 kyr). The data strongly suggest that it is possible to mobilize small degrees of partial melt, in the range of 0.1%. Such small melt fractions may coalesce and move by compaction[4] if the lithosphere experiences local deformation such as shear associated with melting, as is believed to occur in the asthenosphere[5]. □

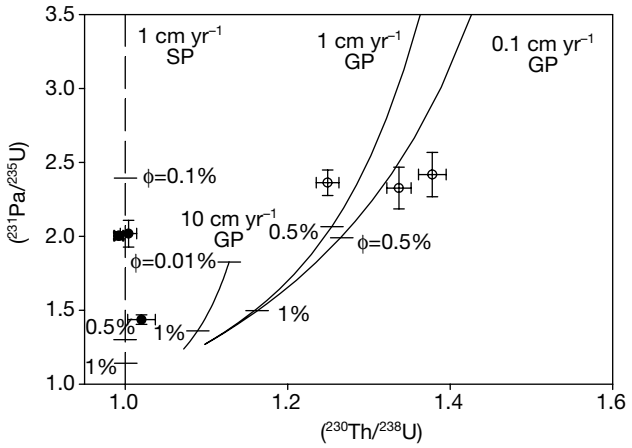

Figure 3 Results from dynamic melting calculations using an equilibrium porous flow model[24] and D values from ref. 19. We have used a 10-km melting column at a maximum F value of 3%. Porosities (ϕ) are shown as tick marks. The model of ref. 24 gives larger enrichments for a given porosity values at upwelling rates of more than 0.1 cm yr^{-1} than the models of refs 23 and 26 (not shown); these two models are indistinguishable at upwelling rates of less than 0.1 cm yr^{-1}. Dynamic melting of a garnet peridotite source is probably appropriate for the asthenosphere derived lavas, similar to MORB, in which melting occurs as a result of decompression melting. Dynamic melting results in larger enrichment compared to static melting, such as batch melting, for equivalent F values. The initial ratios are plotted to show that the degrees of enrichment seen in the samples are possible using physically reasonable upwelling rates and melt porosities. SP, spinel lherzolite; GP, garnet peridotite.

Received 26 October 1999; accepted 8 June 2000.

1. Leeman, W. P. & Harry, D. L. A binary source model for extension-related magmatism in the Great Basin, western North America. *Science* **262,** 1550–1554 (1993).
2. Asmerom, Y. The Th-U fractionation and mantle structure. *Earth Planet. Sci. Lett.* **166,** 163–175 (1999).
3. Asmerom, Y. & Edwards, R. L. U-series isotope evidence for the origin of continental basalts. *Earth Planet. Sci. Lett.* **134,** 1–7 (1995).
4. Kohlstedt, D. L. & Zimmerman, M. E. Rheology of partially molten mantle rocks. *Annu. Rev. Earth Planet. Sci.* **24,** 41–62 (1996).
5. McKenzie, D. The generation and compaction of partially molten rock. *J. Petrol.* **25,** 713– 765 (1984).
6. Pickett, D. A. & Murrell, M. T. Observations of ^{231}Pa/^{235}U disequilibrium in volcanic rocks. *Earth Planet. Sci. Lett.* **148,** 259–271 (1997).
7. Perry, F., Baldridge, W. & DePaolo, D. Role of asthenosphere and lithosphere in the genesis of Late Cenozoic basaltic rocks from the Rio Grande rift and adjacent regions of the southwestern United States. *J. Geophys. Res.* **92,** 9193–9213 (1987).
8. Menzies, M., Kyle, P., Jones, M. & Ingram, G. Enriched and depleted source components for tholeiitic and alkaline lavas from Zuni-Bandera, New Mexico: inferences about intraplate processes and stratified lithosphere. *J. Geophys. Res.* **96,** 13645–13671 (1991).
9. Lynch, D. J., Musselman, T. E., Gutmann, J. T. & Patchett, P. J. Isotopic evidence for the origin of Cenozoic volcanic rocks in the Pinacate volcanic field, northwestern Mexico. *Lithos* **29,** 295–302 (1993).
10. Goldstein, S. J., Murrell, M. T. & Williams, R. W. ^{231}Pa and ^{230}Th chronology of mid-ocean ridge basalts. *Earth Planet. Sci. Lett.* **115,** 151–159 (1993).
11. Lundstrom, C. C., Gill, J., Williams, Q. & Hanan, B. B. Investigating solid mantle upwelling beneath mid-ocean ridges using U-series disequilibria. II. A local study at 33 °S Mid-Atlantic Ridge. *Earth Planet Sci. Lett.* **157,** 167–181 (1998).

© 2000 Macmillan Magazines Ltd

12. Bourdon, B., Joron, J.-L., Christelle, C.-I. & Allegre, C. J. U-Th-Pa-Ra systematics for the Grande Comore volcanics; melting processes in an upwelling plume. *Earth Planet Sci. Lett.* **164,** 119–133 (1998).
13. Thompson, G. A. & Zoback, M. L. Regional geophysics of the Colorado Plateau. *Tectonophysics* **61,** 149–181 (1979).
14. Alibert, C. Peridotite xenoliths from western Grand Canyon and the Thumb; a probe into the subcontinental mantle of the Colorado Plateau. *J. Geophys. Res.* **99,** 21605–21620 (1994).
15. Robinson, J. A. & Wood, B. J. The depth of the spinel to garnet transition at the peridotite solidus. *Earth Planet Sci. Lett.* **164,** 277– 284 (1998).
16. Beattie, P. Uranium–thorium disequilibria and partitioning on melting of garnet peridotite. *Nature* **363,** 63–65 (1993).
17. LaTourrette, T. Z., Kennedy, A. K. & Wasserburg, G. J. Thorium-uranium fractionation by garnet: Evidence for a deep source and rapid rise of oceanic basalts. *Science* **261,** 739–742 (1993).
18. Lundstrom, C. *et al*. Compositional controls on the partitioning of U, Th, Ba, Pb, Sr and Zr between clinopyroxene and haplobasaltic melts: implications for uranium series disequilibria in basalts. *Earth Planet. Sci. Lett.* **128,** 407–423 (1994).
19. Salters, V. J. M. & Longhi, J. Trace element partitioning during the initial stages of melting beneath mid-ocean ridges: *Earth Planet. Sci. Lett.* **166,** 15–30 (1999).
20. Wood, B. J., Blundy, J. D. & Robinson, J. A. The role of clinopyroxene in generating U-series disequilibrium during mantle melting. *Geochim. Cosmochim. Acta* **63,** 1613–1620 (1999).
21. LaTourrette, T. Z. & Burnett, D. S. Experimental determination of U and Th partitioning between clinopyroxene and natural and synthetic basaltic liquid. *Earth Planet. Sci. Lett.* **110,** 227–244 (1992).
22. Hirschmann, M. M. & Stolper, E. M. A possible role for garnet pyroxenite in the origin of the "garnet signature" in MORB. *Contrib. Mineral. Petrol.* **124,** 185–208 (1986).
23. Williams, R. W. & Gill, J. B. Effect of partial melting on uranium decay series. *Geochim. Cosmochim. Acta* **53,** 1607–1619 (1989).
24. Spiegelman, M. & Elliott, T. Consequences of melt transport for uranium series disequilibrium in young lavas. *Earth Planet. Sci. Lett.* **118,** 1–20 (1993).
25. Navon, O. & Stolper, E. Geochemical consequences of melt percolation: the upper mantle as a chromatographic column. *J. Geol.* **95,** 285–307 (1987).
26. McKenzie, D. (^{230}Th/ ^{238}U) disequilibrium and the melting process beneath ridge axes. *Earth Planet. Sci. Lett.* **72,** 81–91 (1985).
27. Riter, J. C. A. & Smith, D. Xenolith constraints on the thermal history of the mantle below the Colorado Plateau. *Geology* **24,** 267–270 (1996).
28. Pickett, D. A., Murrell, M. T. & Williams, R. W. Determination of femtogram quantities of protactinium in geologic samples by thermal ionization mass spectrometry. *Anal. Chem.* **66,** 1044–1049 (1994).
29. Edwards, R. L., Cheng, H., Murrell, M. T. & Goldstein, S. J. Protactinium-231 dating of carbonates by thermal ionization mass spectroscopy: implications for the causes of Quaternary climate change. *Science* **276,** 782–786 (1997).

Acknowledgements

We thank V. Salters, C. Lundstrom and D. Pickett for comments on the manuscript and M. Spiegelman, M. Reagan and D.L. Kohlstedt for discussions. We also thank the US Park Service for access. This work was and is being supported by the US National Science Foundation.

Correspondence and requests for materials should be addressed to Y.A. (e-mail: asmerom@unm.edu).

Female bluethroats enhance offspring immunocompetence through extra-pair copulations

Arild Johnsen*, Vegard Andersen, Christine Sunding & Jan T. Lifjeld*

Zoological Museum, University of Oslo, Sars gate 1, N-0562 Oslo, Norway

Female birds frequently copulate with extra-pair males[1,2], but the adaptive value of this behaviour is poorly understood[2]. Some studies have suggested that 'good genes' may be involved, where females seek to have their eggs fertilized by high-quality males without receiving any material benefits from them[3,4]. Nevertheless, it remains to be shown that a genetic benefit is passed on to offspring[5,6]. Here we report that nestling bluethroats, *Luscinia svecica*, sired by extra-pair males had a higher T-cell-mediated immune response than their maternal half-siblings raised in the same nest. The difference could not be attributed to nestling body mass, sex or hatching order, but may be an effect of paternal genotype. Extra-pair young were also more immunocompetent than their paternal half-sibs raised in the genetic father's own nest, which indicates an additional effect of maternal genotype. Our results are consistent with the idea that females engage in extra-pair copulations to obtain compatible viability genes, rather than 'good genes' *per se*.

Extra-pair mating systems are highly suitable for the study of genetic benefits of mate choice. When eggs in a clutch are fertilized by both the social male and one or more extra-pair males, the effect of paternal genes on offspring fitness can be assessed directly by comparison of maternal half-sibs[6]. This is because the sib groups share the same rearing environment and genes from the mother. The test prediction from 'good genes' models is then that extra-pair young (EPY) should perform better than within-pair young (WPY) raised in the same brood. Moreover, if females choose compatible male genes in extra-pair mate choice, it follows that EPY should also perform better than their paternal half-sibs, that is, the WPY of the extra-pair male. Here we have tested these predictions in a population of wild bluethroats where extra-pair paternity occurs at a relatively high frequency[7,8].

We studied cell-mediated immunity in nestling bluethroats by a subcutaneous injection of phytohaemagglutinin (PHA) in one

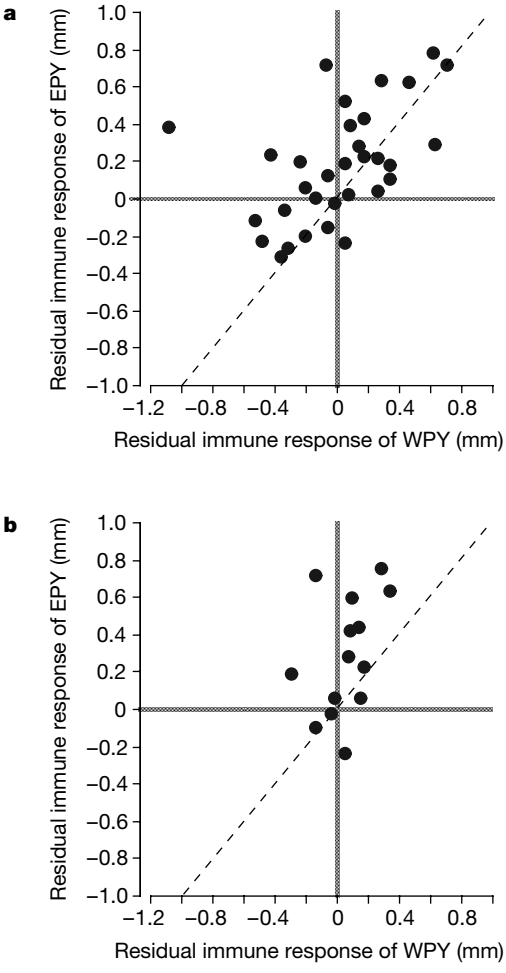

Figure 1 Relationships between residual phytohaemagglutinin (PHA) response of extra-pair young (EPY) and within-pair young (WPY) in bluethroat broods, after controlling for nestling body mass. **a**, Maternal half-sibs raised in the same nest ($n = 32$). **b**, Paternal half-sibs raised in different nests ($n = 14$). Points indicate brood means. Diagonal dashed lines represent identical responses of EPY and WPY.

* Present addresses: Department of Zoology, Göteborg University, PO Box 463, S-405 30 Göteborg, Sweden (A. J.); Department of Biological Sciences, Lapham Hall, PO Box 413, University of Wisconsin Milwaukee, WI 53201, USA (J. T. L.).

© 2000 Macmillan Magazines Ltd